New insight techniques to analyze rock-slope relief using DEM and 3D-imaging cloud points: COLTOP-3D software

Chapter · May 2007

DOI: 10.1201/NOE0415444019-c8

Michel Jaboyedoff
University of Lausanne

Thierry Oppikofer
Norges geologiske undersøkelse

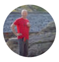

Marc-Henri Derron
University of Lausanne

Jacques Locat
Laval University

UNIL | University of Lausanne
Faculty of Geosciences and Environment
Institute of Geomatics and Risk Analysis
Amphipôle
CH-1015 Lausanne

Reprint

Jaboyedoff M., Metzger R., Oppikofer T., Couture R., Derron M.-H., Locat J. Turmel D. (2007): New insight techniques to analyze rock-slope relief using DEM and 3D-imaging cloud points: COLTOP-3D software. In Eberhardt, E., Stead, D and Morrison T. (Eds.): Rock mechanics: Meeting Society's Challenges and Demands (Vol. 1), Taylor & Francis. pp. 61-68.

This version contains colour figures that were printed in greyscale in the conference proceedings of the 1st Canada-US Rock Mechanics Symposium, Vancouver, Canada, 27-31 May 2007.

Faculty of Geosciences and Environment
Institute of Geomatics and Risk Analysis

Phone +41 21 692 35 32 | Fax +41 21 692 35 35 | Michel.Jaboyedoff@unil.ch

New insight techniques to analyze rock-slope relief using DEM and 3D-imaging cloud points: COLTOP-3D software

M. Jaboyedoff, R. Metzger &T. Oppikofer
IGAR Institute of Geomatics and Risk Analysis, FGSE - University of Lausanne, Switzerland

R. Couture
Geological Survey of Canada, Ottawa, Ontario, Canada

M.-H. Derron
Geological Survey of Norway, International Center for Geohazards, Trondheim, Norway

J. Locat & D. Turmel
Université Laval, Québec, Canada

ABSTRACT: COLTOP-3D software performs structural analysis of a topography using a digital elevation model (DEM). A color is defined based on slope aspect and slope angle in order to obtain a unique color code for each spatial orientation. Thus continuous planar structures appear as a unique color. Several tools are included to create stereonet(s), to draw traces of discontinuities, or to compute automatically density stereonet. A new version has recently been developed to represent true 3D surfaces from point clouds. Examples are shown to demonstrate the efficiency of the method. High resolution DEMs acquired with Lidar techniques greatly improve topographic analyses.

1 INTRODUCTION

Digital elevation models (DEMs) are used in many hazard assessment methods, including landslides and rock instabilities. Slope angles are used for stability estimation, e.g. infinite slope stability models (Dietrich et al., 2001). Kinematic tests are used to estimate the likelihood of failure in rock slopes, such as slide, wedge and toppling failures (Jaboyedoff et al., 2004; Gokceoglu et al., 2000; Günther, 2000). DEMs are also used for modeling rockfall trajectories.

Many GIS tools permit a mathematical analysis of topography using slope, slope aspect, second derivative, curvature, flow paths, etc. (Burrough and McDonnell, 1998). But very few are dedicated to the analysis of the relief structure. An attempt of merging slope angle and slope aspect in one document was made by Brewer and Marlow (1993) to represent topography using colors dependent on both slope angle and slope aspect, but the results were not used for structural analysis. Using the dip and strike direction of each cell, a DEM can be theoretically represented with a map having a unique color for each spatial orientation, allowing a very simple slope analysis. This can also be applied to triangulated surfaces made from 3D point clouds (i.e. x, y, z, coordinates), should define, enabling for example, the detection of planar structures within a cliff.

The increasing availability and accuracy of high resolution DEMs by Lidar (LIght Detection And Ranging) technologies allow for more detailed structural and morphological analyses and increase the potential of DEM analyses. Although if the principle of the proposed analysis is simple, the point cloud management and surface creation is not straightforward.

In this paper we describe the principle of COLTOP -3D software, its use for DEM analysis and its future evolution toward a true 3D analysis. This is illustrated with some examples from rock cliffs in Québec and in the Swiss Alps.

2 METHOD

2.1 *Document types*

Airborne Lidar DEMs have been available for more than 10 years, either as point clouds or regular grids. Up to now most of the acquisitions have been performed with a nearly vertical laser beam, which means that the cliffs are only poorly defined because of a poor point density. The new techniques linked to ground-based Lidar permit the creation of accurate 3D images by merging several scans. By combining the two technologies it is possible to obtain a point cloud that has no preferential density direction (Fig. 1), which means that the topographic surfaces have similar point densities in all spatial directions.

The ground-based Lidar data often include vegetation, which must be removed manually. The interest is also to create a routine to automatically remove the trees from scans.

2.2 *Software principle*

The first version of COLTOP-3D (Jaboyedoff and Couture, 2003) displays a square DEM grid using the Hue Saturation Intensity (HSI) wheel. The color displayed is linked directly to direction of the normal (pole) of the DEM cells by representing the HSI wheel, in a stereonet and showing the link between pole orientation and colors (Fig. 2). The dip direction of the surface elements are represented by the hue (H) of the wheel from 0 to 360° and the dip of the pole using the saturation (S). The intensity (I) can be changed for representation purposes. The link with RGB value is performed following the relationship proposed by Gonzalez et al. (2004).

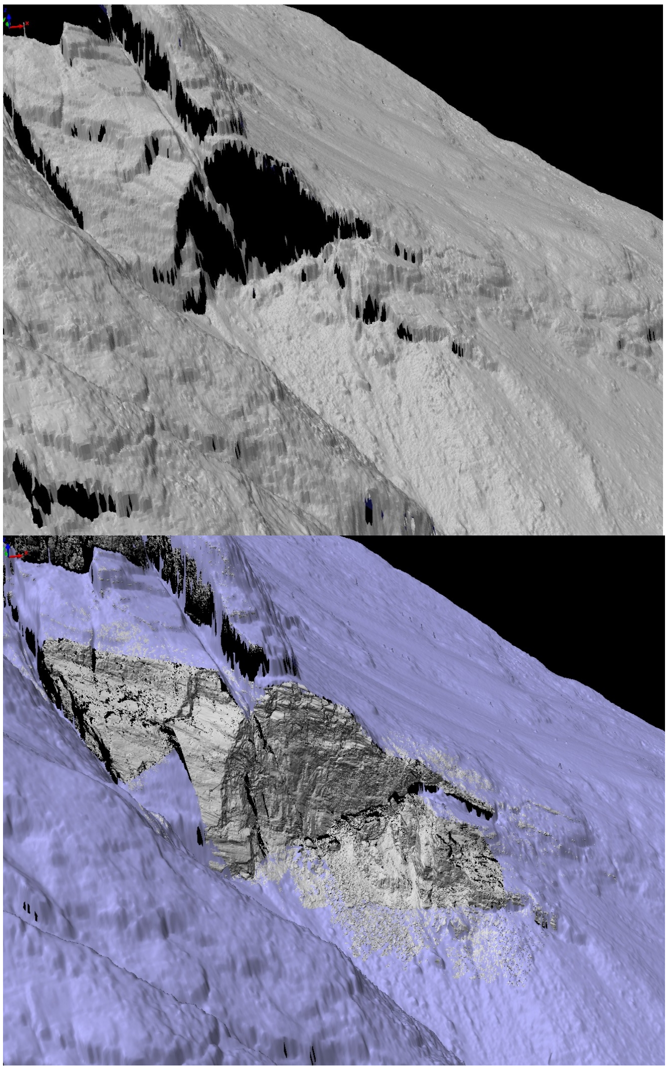

Figure 1. Example of an airborne Lidar DEM on top, and the merge of the ground-based and airborne Lidar DEM on the bottom (DEM from Åknes project, Stranda Commune, Norway; after Derron et al., 2005).

2.3 *The 2D representation*

Basically, COLTOP-3D was designed to use square grids. Contrary to standard methods, the colored pixels are created by using the normal of the plane defined by 4 neighboring grid points and by placing the HSI value corresponding to the normal vector orientation at the center of these points (Fig. 2). If the grid's cell size is d and the four points' altitudes are z1, z2, z3 and z4, then the surface orientation can be defined by two following vectors:

$$\vec{v}_1 = \left[d \;\; ;0 \;\; ;½(z_1 + z_3 - z_2 - z_4)\right] \quad (1)$$

$$\vec{v}_2 = \left[0 \;\; ;d \;\; ;½(z_1 + z_2 - z_3 - z_4)\right] \quad (2)$$

They correspond to the line passing through the center of the cell and linking the middle of the edges defined by the segment linking the 4 grid points. The pole is given by the cross product:

$$\vec{p} = \vec{v}_1 \times \vec{v}_2 \quad (3)$$

Another solution has been used to represent surfaces created by TIN (triangulated irregular network) techniques by simply applying the color respecting the above method to each triangle.

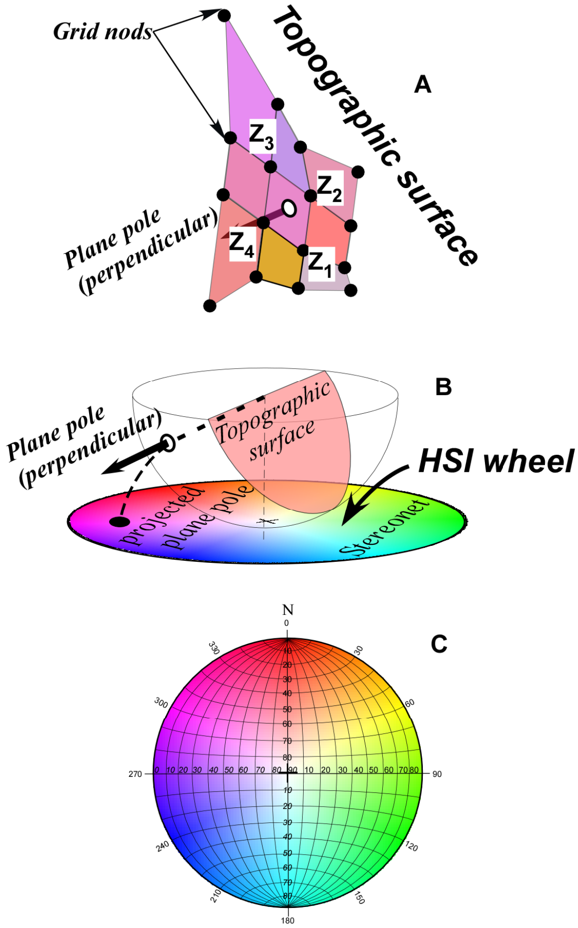

Figure 2. Illustration of the principle of the COLTOP-3D color scheme. (A) The orientation is defined by four nearest neighbors on a square grid or by three points of each triangle of a TIN. (B) Relationship between Schmidt-Lambert projection and HSI wheel. (C) The HSI wheel plotted on a stereonet that is afterward affected to the cells of A..

2.4 *Other capabilities*

COLTOP-3D possesses several others capabilities besides the simple representation by means of the HSI wheel (Fig. 3). The color scheme can be also rotated in order to get a better visualization of different planar features. Since the color is a direct indicator of the orientation, one can select and click on a colored pixel and instantaneously the dip angle and dip direction is returned. By clicking on the image, the standard sign of dip is plotted on the colored DEM and the corresponding orientation is added to a stereonet and listed in a text window.

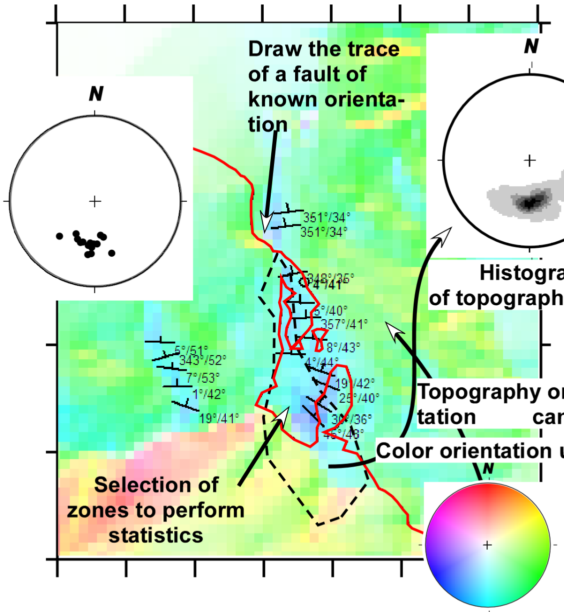

Figure 3. Illustration of the capabilities of COLTOP-3D designed for a square grid DEM (The image is normally in color, see data repository).

By selecting an area of the DEM, it is possible to calculate the histogram of the orientations (density stereonet), for example to obtain the mean orientation of a planar surface. The DEM cells for which the orientations corresponds to a chosen orientation (defined by a dip angle, a dip direction and a tolerance (cone) around this orientation) can be mapped in a single color. By choosing up to five different orientations, this leads to an image of the relief displaying only the selected orientations with user-defined colors. Results can be exported in an ASCII grid file that can be used in any common Geographic Information System (GIS) software.

Currently fault traces can be drawn in COLTOP-3D by indicating one point and the orientation of the fault or by clicking on 3 points. Further developments will implement least-square methods for the determination of fault traces. The X-Y coordinates of fault traces can be exported into a text file.

3 THE TRUE 3D REPRESENTATION

3.1 *3D point cloud data management*

Ground-based laser scanners allow for capturing dense 3-dimensional data sets (up to millions of points) of the surface of an object, within a few minutes. However, the post-treatment and the standard operating use of such large data sets may impair an in-depth analysis for specific applications, such as landslide and rockfall analysis. This is mainly due to computer access time for the localization of data points near a given location. To solve these problems, a structure based on octrees (an index based on spatial portioning) is used, which allows for fast localization of points within a given region, low consumption of RAM, and hard drive access minimization. First a region (root node) large enough to enclose the entire point cloud is computed. Points are added one by one until the root node (level 0) contains a total number of point equals to a given threshold. The node is then equally splitted into eight sub regions (sub nodes) (level 1), and all points of the root node are removed and added to their corresponding sub nodes. This subdivision process is repeated until the number of points included in a sub node falls beneath a given threshold. The value of the threshold must be large enough, typically in the order of few hundreds of thousand, for fast disk access, as all the points contained in a sub node are automatically loaded into RAM and unloaded from it as a whole. Figure 4 (top) shows an example of a first order octree (only non-empty nodes are shown) This first octree allow not only for minimizing disk access, but also for minimizing RAM consumption.

For solving hardware problems related to 3D point topology, a second octree is built as described above, but with a much smaller threshold: typically it is in the order of a few hundreds to one thousand. This leads to an octree with much more branches (Fig. 4b).

The retrieval of neighborhood points of a given coordinate (x,y,z) is then straightforward. First, the node of the first octree holding (x,y,z) is retrieved, and, if needed, the data points are loaded into RAM. Secondly, the procedure is repeated for the second octree. The few hundreds of points stored in this node are inspected to obtain the nearest neighbors of (x,y,z).

This structure is similar to the ones proposed by Dey and al. (2001) and Schaffer and Garland (2005).

3.2 *Normal estimation*

Extensive work has pinpointed that eigenvalue analysis of the covariance matrix of a local neighborhood can be used to determine local surface properties, and hence its normal vector (Pauly et al., 2002). The covariance matrix ***C*** is defined over a local neighborhood surrounding a point of interest as:

$$C = COV(X) = \begin{bmatrix} \sigma_{xx} & \sigma_{xy} & \sigma_{xy} \\ \sigma_{xy} & \sigma_{yy} & \sigma_{yz} \\ \sigma_{xz} & \sigma_{yz} & \sigma_{zz} \end{bmatrix} \quad (4)$$

where the entries for a neighborhood containing k points are defined as:

$$\sigma_x^2 = \text{var}(x) = E(x^2) - E(x)^2 = \frac{1}{k}\sum_{i=1}^{k}(x_i - \bar{x})^2 \qquad (5)$$

$$\sigma_{xy} = \text{cov}(x,y) = E(xy) - E(x)E(y) = \frac{1}{k}\sum_{j=1}^{k}(x_i - \bar{x})(y_i - \bar{y}) \qquad (6)$$

with *E(value)* being the excepted value or the mean value (*E(x)=x*), and *var(x)* and *cov(x,y)* denoting the variance of *x* and the covariance between *x* and *y* respectively (Belton and Lichti, 2002).

Since ***C*** is a symmetric and positive semi-definite, its associated eigenvalues λ_i are greater than or equal to zero. The local normal vector is given by the associated eigenvector e_i with the smallest eigenvalue. The direction of the normal vector is the same as the one found by least squares plane fitting, since the two methods are equivalent (Shakarji, 1998).

3.3 Removing of non-surface features

One of the main advantage of computing eigenvalues for normal estimation instead of least-squares plane fitting, is that the eigenvectors correspond to the principal components (directions and orientations) of the neighborhood and the eigenvalues will represent the variance in each direction (Belton and Lichti, 2002). Thus, it is possible to estimate the change of geometric curvature, M_{curv}, in the neighbourhood of a single point, p_i, with simple calculation such as (Bae and Lichti, 2004):

$$M_{curv}(p_i) = \frac{\lambda_1}{\lambda_1 + \lambda_2 + \lambda_3} \quad \text{with } 0 \le \lambda_1 \le \lambda_2 \le \lambda_3 \qquad (7)$$

Points lying on the surface will have a change of curvature value close to zero. Belton and Lichti (2002) use the values given by eq. 7 to classify the points as surface (plane), edges or corners (their field of application being terrestrial laser scans of buildings). From a slope instability or rockfall hazard analysis point of view, these features do not have a particular meaning, but the change of curvature can be used to automatically remove vegetation from the data set, as it is excepted that such features have a highly variable curvature. Depending on the scanned area, it takes up to one day to manually remove trees from a single scan. Vegetation and foliage are automatically detected by specifying a threshold for the values given by eq. 7. Points with higher curvature than the threshold can be removed from the dataset (Fig. 5). However, the procedure is not as straightforward, as it can be seen from Figure 5. Some surfaces or ground points located on a fracture or fault may also be deleted by blindly applying the filter.

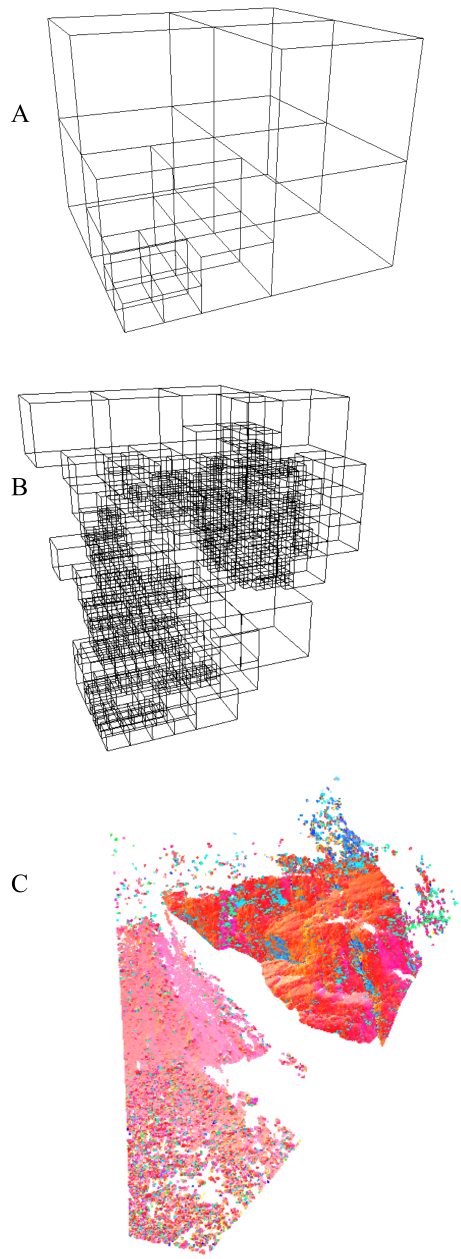

Figure 4: First order octree (A), second order octree (B) and original data set of the Randa rockfall (C).

3.4 Surface reconstruction

Surface reconstruction is a topic of great interest in the computer graphics field and there are numerous works regarding surface reconstruction. Amenta and Bern (1998) give a short review of the most popular algorithms.

The surface reconstruction is very important for landslide or rock instability studies, since it allows firstly for the automatic delineation of faults, and secondly for visibility culling purposes, as points in the background may make the interpretation difficult.

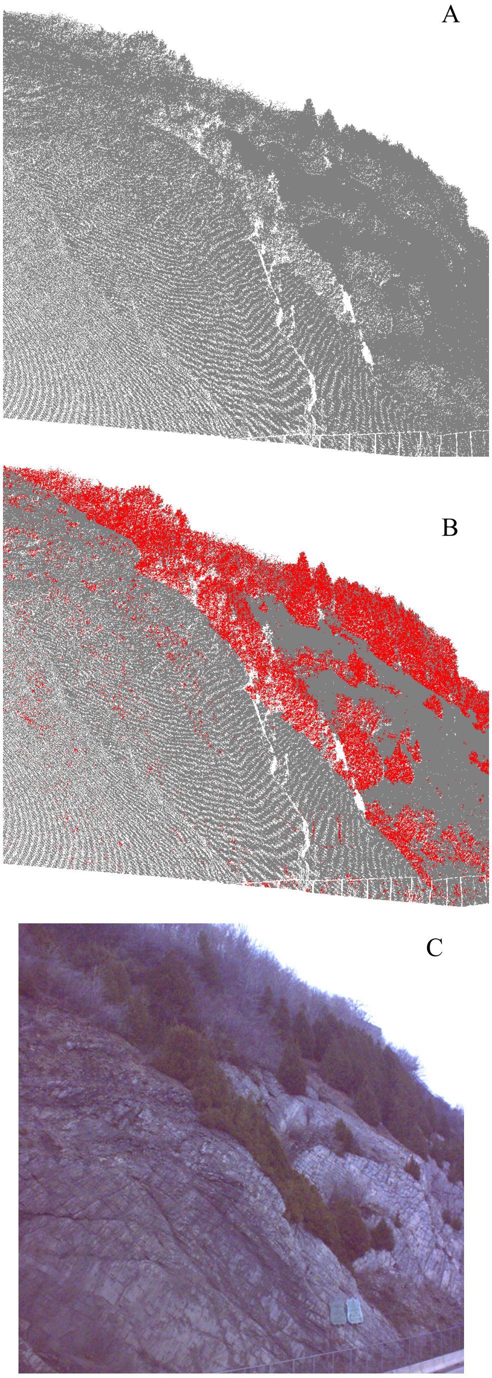

Figure 5. Original point cloud (A), vegetation points highlighted in red (B) and picture of the scanned area (C) (Boulevard Champlain, Quebec City, Canada).

Most, if not all, of the surface reconstruction algorithms imply that the surface to reconstruct is smoothed and that the sampling density is fine enough to capture all its features. However, this assumption can often not be met on the scanned rock surfaces, due to the intrinsic roughness of the study site and/or the distance from the ground-based Lidar device to the target (up to 1,000 m), which may lead to an undersampling and the missing of small scale features. Moreover, the collected data points may easily reach values on the order of millions, impairing most of the standard algorithms (Shaffer and Garland, 2005). To overcome these problems, a local reconstruction algorithm similar to the one proposed by Linsen and Prautzsch (2001) is used. For each point p, all the points within a user-defined, 3D radius are retrieved ($p_1,\ldots,p_k$). The k points are then projected on the plane defined by p and its normal. A local coordinate system transformation allows for 2D Delaunay triangulation (Delaunay, 1934). The n triangles, which hold point p as a vertex, are inserted in the global triangle surface list, the others being dismissed. Our experience shows that n should be in the range of 5 to 7, which is consistent with well distributed points. As stated by Linsen and Prautzsch (2001), local reconstruction does not ensure the topological correctness of the surface, but a post filtering process can easily overcome this problem. Starting from using the above triangulation method, the surface can be represented with COLTOP-3D color scheme (Fig. 6).

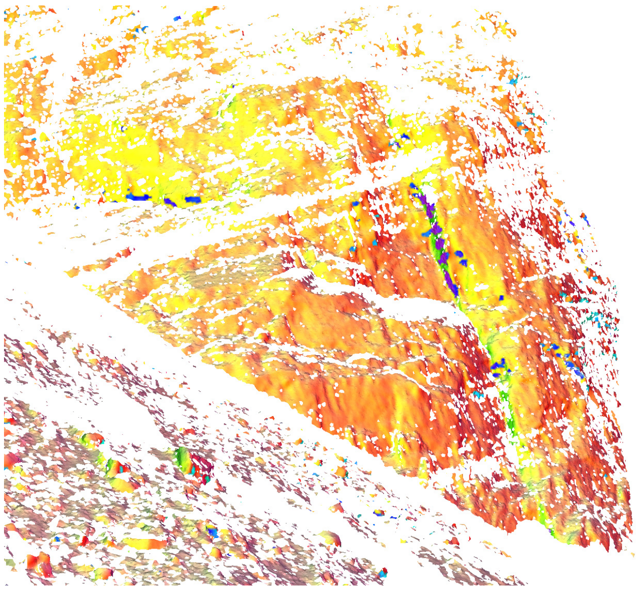

Figure 6. Surface reconstruction of a scattered points cloud of the Randa rockfall. The colors correspond to the dip angle and dip direction of the surfaces.

4 EXAMPLE

To illustrate an application of COLTOP-3D, we present the analysis of a mountain peak in the Swiss Alps, Grand Muveran summit (3051 m a.s.l.). This peak is transected by long faults that are very difficult to measure directly on the field, because they affect the relief at a small scale. Furthermore, such summits are not easy to survey without perilous climbing efforts (Figure 7A). As shown on Figure 8, these large faults generate rock instabilities within the cliffs.

The analysis performed with COLTOP-3D indicates that the fault slopes have a mean dip direction of 205° and a mean dip angle of 45°. The DEM cells, whose orientation are within a tolerance of ±20° around this mean direction can be exported into a GIS file. The results (Figure 9) show that the west facing slope is clearly shaped by these discontinuities (Figures 7 and 9).

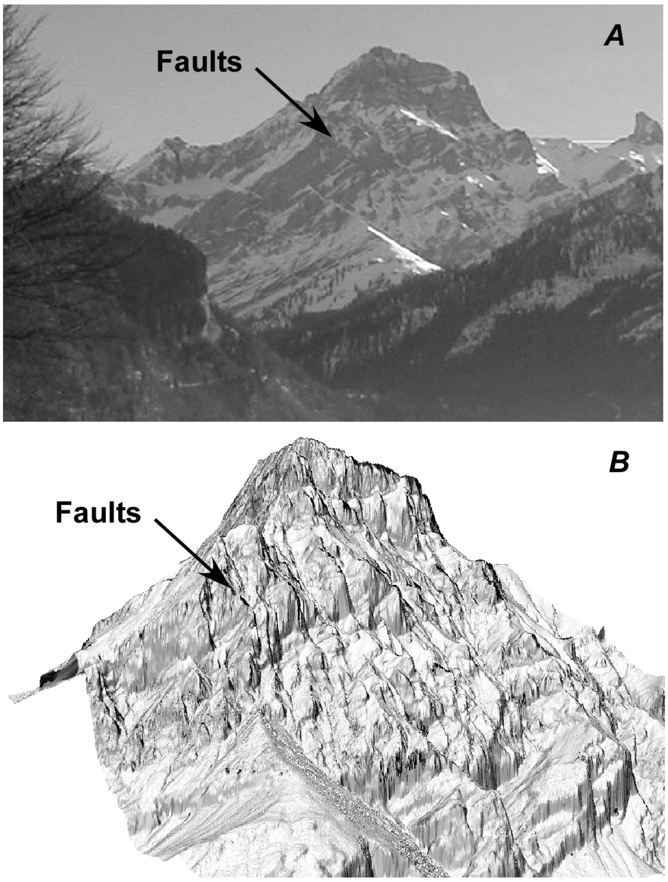

Figure 7. View of the west face of the Grand Muveran summit displaying sets of faults on picture (A) and on the 1 m resolution airborne laser-DEM represented by a 3D shaded relief in (B) (Source: MNT-MO/MNS, (c) 2007 SIT).

This shows that it is very easy to obtain structural data using aerial Lidar DEM. This example also shows the need to acquire data with ground based Lidar in order to study the instabilities within the cliffs. For example, the instability shown in Figure 8 needs to be analyzed in detail by terrestrial Lidar and the new COLTOP-3D version.

- In the basement rock of the Swiss Alps, the fracturing is well enough developed to shape up to 50% of the slope orientations, or even more at outcrop scale. Often the entire slope is controlled by two or three main discontinuity sets (Jaboyedoff et al., 2004).
- Structural analysis of the scar of Frank Slide (Canada) permitted to refine previous interpretations (Jaboyedoff et al., in press).
- Recent works on the Eiger collapse in Switzerland clearly show the control of structures, and that 3D point clouds are needed to understand the mechanism of rock instabilities (Oppikofer et al., in prep.).


Figure 8. Example of rock slope instability scar (in yellow-beige) controlled by the faulting system shown in Figure 7.

The efficiency of of the COLTOP color representation of the relief has also been illustrated by the following examples:

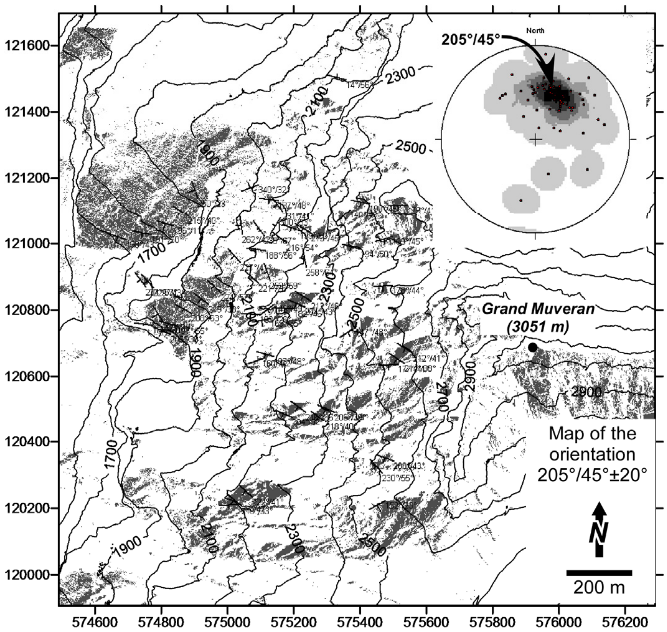

Figure 9. Application of COLTOP-3D to the Grand Muveran summit. The faults shown in Figure 7 (mean dip direction and dip angle is 205°/45°) are identified in grey.

5 DISCUSSIONS AND CONCLUSION

3D point clouds from airborne or ground-based Lidar recordings permit a rapid structural analysis. This is useful since joints and instabilities are often in inaccessible zones.

The colors obtained from grid DEMs using the Hue Saturation Index in COLTOP-3D permit an easy detection of the main features of a relief, such as the main joint sets shaping rock faces. The colored surfaces and their interactivity, allow for a detailed structural analysis.

Unstructured clouds of 3D data points can serve as a basis for surface reconstruction by triangulation.

Thus, the color representation, based on the dip direction and the dip angle of the surface, can be assigned to each triangle. This color representation forms a simple way to quickly obtain information for slope analysis. COLTOP-3D has shown its efficiency using square DEM grids. The difficulty to implement a true 3D version comes from: (1) storage and access of huge Lidar data sets; (2) octree classification and triangulation of data points; (3) extraction of 3D surface resulting from the triangulation, and; (4) representation of the 3D surface according to a Hue Saturation Index wheel using the dip direction and dip angle.

The promising preliminary results presented here indicate that these new DEM analysis tools will greatly help structural geologists and rock mechanics engineers by supplementing part of the classical field work and permitting to contribute to more quantitative field work analysis.

The use of both grid DEM and point clouds open a lot of new perspectives in relief interpretation as suggested in the above examples. The field work will be greatly improved by the preliminary DEM investigations in the office.

Since the power of computer will still increase in the next years, permitting the management of huge datasets, letting us think that the future is “cloudy”.

AKNOWLEDGMENTS

We thank the Åknes Project (Stranda Commune, Norway) and its leader Dr. L. Blikra for providing the DEM in Figure 1. D. Conforti and B. Ysseldyk from Optech Corp. are thanked for their kind collaboration. We thank also the Canton de Vaud (Switzerland) for providing DEM data of the Grand Muveran region. We thank anonymous reviewers for their help in improving this manuscript, especially the GSC internal reviewer.

REFERENCES

Agliardi, F. and Crosta, G., 2003. High resolution three-dimensional numerical modelling of rockfalls. Int. J. Rock Mech. and Mining Sci., 40, 455-471.

Amenta, N. and Bern, M. 1999, Surface reconstruction by Voronoi filtering, Discrete & Computational Geometry, vol 22-4.

Bae, K.-H. and Lichti, D. 2004. Edge and Tree Detection from Three-dimensional Unorganised Point Clouds from Terrestrial Laser Scanners, Proceedings of the 12th Australian Remote Sensing and Photogrammetry Conference, October, Fremantle, WA, CD-ROM, 9pp.

Belton, D. and Lichti, D. 2005. Classification and Feature Extraction of 3D Point Clouds from Terrestrial Laser Scanners, in SSC2005: Spatial Intelligence, Innovation and Praxis: Proceedings of National Biennal Conference of the Spatial Sciences Institute 2005, Melbourne, Vic, pp. 39-48, CD Publication.

Brewer, C. A. and Marlow, K. A. 1993, Color representation of aspect and slope simultaneously. Proceedings, Eleventh International Symposium on Computer-Assisted Cartography (Auto-Carto-11), Minneapolis, 328-337.

Burrough, P.A. and McDonnell, R.A., 1998. Principles of geographical information systems. Oxford University Press, Oxford, 333 p.

Delaunay, B. 1934, Sur la sphère vide, Bul Acad Sci URSS, 793-800

Derron, M.H., Blikra, L.H. and Jaboyedoff, M. 2005. Norway High Resolution Digital Elevation Model Analysis for Landslide Hazard Assessment (Åkerneset, Norway). In: Senneset, K., Flaate, K. and Larsen, J.A:: Landslide and avalanches, ICFL 2005. 101-106.

Dey, T.K., Giesen, J. and Hudson, J. 2001. Delaunay based shape reconstruction from large data. Proc. IEEE Symposium in Parallel and Large Data Visualization and Graphics (PVG2001), 19-27.

Dietrich, W.E., Bellugi, D. and de Asua, R. 2001. Validation of the shallow landslide model, SHALSTAB, for forest management. In Wigmosta, M.S. and Burges, S. J. (eds), Land Use and Watersheds: Human influence on hydrology and geomorphology in urban and forest areas; Amer. Geoph. Union, Water Science and Application, 195-227.

Gokceoglu, C., Sonmez, H. and Ercanoglu, M. 2000. Discontinuity controlled probabilistic slope failure risk maps of the Altindag (settlement) region in Turkey, Eng. Geol., 55, 277–296.

Gonzalez, R.C., Woods, R. and Eddins, S. 2004. Digital Image Processing Using Matlab. Prentice Hall, pp. 624.

Günther, A. 2003. SLOPEMAP: programs for automated mapping of geometrical and kinematical properties of hard rock hill slopes, Computers and Geosciences, 29/7, 865–875.

Jaboyedoff, M. and Couture, R. 2003. Report on the project COLTOP3D for March 2003: stay of Michel Jaboyedoff at GSC - Ottawa. Quanterra administrative document - Activity report - RA01.

Jaboyedoff, M., Baillifard, F., Couture, R., Locat, J. and Locat, P. 2004. New insight of geomorphology and landslide prone area detection using DEM. In: Lacerda, W.A., Ehrlich. M. Fontoura, A.B. and Sayo. A (eds): Landslides Evaluation and stabilization. Balkema, 191-197.

Jaboyedoff, M., Baillifard, F., Philippossian, F. and Rouiller, J.-D. 2004. Assessing the fracture occurrence using the "Weighted fracturing density": a step towards estimating rock instability hazard. Natural Hazards and Earth System Sciences, 4, 83-93.

Jaboyedoff M, Couture, R. and Locat, P. in press. Structural analysis of Turtle Mountain (Alberta) using digital elevation model: toward a progressive failure. Geomorphology.

Linsen, L. and Prautzsch, H. 2001. Local Versus Global Triangulation. EUROGRAPHICS 2001, vol. 20-3.

Oppikofer, T., Jaboyedoff, M. and Keusen, H.-R. in prep. High resolution monitoring and analysis of the Eiger rock slope collapse induced by climate changes.

Pauly, M., Gross, M. and Kobbelt, L. 2002. Efficient Simplification of Point-Sampled Surfaces, IEEE Visualization.

Shaffer, E. and Garland, M. 2005. A multiresolution representation for massive meshes. IEEE Transactions on Visualization and Computer Graphics, 11(2):139–148

Shakarji, C. 1998. Least-Squares Fitting Algorithms of the NIST Algorithm Testing System. Journal of Research of the National Institue of Standards and Technology. Vol. 103, n° 6.